

# Size-, shape-, and composition-dependent polarizabilities of $\text{Si}_m\text{C}_n$ ( $m, n = 1 - 4$ ) clusters

You-Zhao Lan<sup>1</sup> (蓝尤钊)

*Zhejiang Key Laboratory for Reactive Chemistry on Solid Surfaces, Institute of Physical Chemistry, Zhejiang Normal University, Zhejiang, Jinhua 321004, China*

## Abstract

We theoretically investigate the size-, shape-, and composition-dependent polarizabilities of the  $\text{Si}_m\text{C}_n$  ( $m, n = 1 - 4$ ) clusters by using the density functional based coupled perturbed Hartree-Fock method. The size-dependence of the polarizabilities of the  $\text{Si}_m\text{C}_n$  ( $m, n = 1 - 4$ ) clusters is more complicated than that of pure  $\text{Si}_m$  and  $\text{C}_n$  ( $m, n = 1 - 8$ ) clusters because for a given cluster size the heteroatomic clusters have more isomers than the homoatomic ones. For the shape-dependence, we consider three kinds of shape, linear (chain), prolate, and compact. For most clusters, we can clearly observe orders of  $\alpha(\text{linear}) > \alpha(\text{prolate})$  and  $\alpha(\text{prolate}) > \alpha(\text{compact})$  for a given composition. The composition-dependence of polarizabilities reveals that the linear clusters have an obvious larger polarizability than both the prolate and the compact clusters especially for a given  $m/n$  value. The shape effect makes a main contribution to determine the size of the polarizability. To understand the size of polarizability and the evolution of polarizability, we have tried many factors, such as the energy gap and binding energy, and defined a new parameter ( $\Delta q$ ) that characterizes the redistribution of charge in cluster. We find that both the binding energy and the  $\Delta q$  are more available than the energy gap for reflecting the evolution of polarizabilities provided that both the cluster shape and one of the components in cluster are fixed. The correlation between the polarizability and the energy gap is poor, in agreement with the previous results.

PACS numbers: 36.40.-c, 36.40.Vz, 36.40.Cg, 31.15.ap

## 1. Introduction

Clusters have markedly different physical or chemical properties from their corresponding bulk material [1, 2]. For example, the bondings in cluster are different from those in the bulk [3]; the energy gap between the highest occupied molecular orbital (HOMO) and the lowest unoccupied molecular orbital (LUMO) is generally larger than the corresponding bulk value [1]; the linear absorption spectra of the clusters exhibit long absorption tails in the low-transition-energy region and strong absorption peaks in the high-transition-energy region ( $> \sim 4.5$  eV) [4]; the optical polarizabilities of the clusters are very different from those of the bulk material [5, 6], and so on. Investigating the properties of a cluster is all along a topic of interest because we can assess the potential applications of a cluster in nanotechnology.

In the last 20 years, the (hyper)polarizabilities of small semiconductor clusters, such as gallium arsenide (GaAs), silicon (Si), silicon carbide (SiC), and aluminum phosphide (AlP) clusters, have attracted much attention [5 – 31]. Experimental studies have shown that the static polarizabilities of the  $\text{Si}_m$  ( $m = 9 - 50$ ) and  $\text{Ga}_m\text{As}_n$  ( $m + n = 5 - 30$ ) clusters fluctuate around their

---

<sup>1</sup> Corresponding author: Youzhao Lan; Postal address: Zhejiang Key Laboratory for Reactive Chemistry on Solid Surfaces, Institute of Physical Chemistry, Zhejiang Normal University, Jinhua 321004, China; Fax: +086 579 82282269; E-mail address: lyzhao@zjnu.cn

corresponding bulk values [5]. These experimental results have motivated many theoretical studies of the polarizabilities of the Si and GaAs clusters [6, 7, 9, 11 – 14, 20, 30, 31]. Theoretical studies showed that the size of polarizability directly or indirectly depends on many factors such as cluster size, cluster shape, cluster composition, energy gap, binding energy, and ionization potential, and so on. The size-dependence of the polarizabilities has been well known for the Si and GaAs clusters [5 – 7, 9, 11 – 13, 30, 31]. For small  $\text{Si}_m$  ( $m < 10$ ) and  $\text{Ga}_n\text{As}_m$  ( $n + m < 8$ ) clusters, the theoretic polarizabilities are higher than the bulk value and decrease with the increasing cluster size [5 – 7, 14, 20] indicated by the number of atoms in cluster. For mediate-size  $\text{Si}_m$  ( $m = 9 – 50$ ) and  $\text{Ga}_n\text{As}_m$  ( $n + m = 5 – 30$ ) clusters, experimental polarizabilities [5] vary strongly and irregularly with the cluster size and fluctuate around the bulk value. For large  $\text{Si}_m$  ( $m = 60 – 120$ ) clusters, all experimental polarizabilities are lower than the bulk value [5]. However, for the  $\text{Si}_m$  ( $m = 9 – 28$ ) clusters, Deng *et al.* [11] found that theoretical polarizabilities exhibit fairly irregular variations with the cluster size and all calculated values are higher than the bulk value. Similar theoretical results have been also obtained by Sieck *et al.* [25] and Jackson *et al.* [12] for the  $\text{Si}_m$  ( $m = 1, 3 – 14, 20$ , and  $21$ ) and ( $m = 1 – 21$ ) clusters, respectively. Until now the discrepancies between experimental and theoretical polarizabilities have not been well explained [11, 12]. More investigations are required.

The shape-dependence of polarizabilities has been also known for the Si, GaAs, and AlP clusters [9, 12, 27, 32]. For the  $\text{Si}_m$  ( $m = 20 – 28$ ) clusters, the prolate clusters have systematically larger polarizability than the compact ones [9]. This shape-dependence reflects the metallic character of these small clusters because it is reproduced by using the jellium models. For the prolate  $(\text{GaAs})_n$  and  $(\text{AlP})_n$  clusters [26, 27, 32], the (hyper)polarizabilities monotonically increase with an increase of  $n$ . This trend is very similar to the well known (hyper)polarizability evolution of extended conjugated organic molecules [33]. We also notice other interesting shape-dependence of polarizabilities. For the  $\text{Co}_n(\text{C}_6\text{H}_6)_m$  ( $n, m = 1 – 4, m = n, n + 1$ ) clusters [34], the sandwich clusters have systematically larger polarizabilities and anisotropies than the rice-ball isomers, which suggests that we should distinguish these two kinds of clusters in terms of their dipole polarizabilities. The (hyper)polarizabilities of the Möbius, normal cyclacene, and linear nitrogen-substituted strip polyacenes exhibit a clear shape-dependence [35]. The shape-dependence based on the geometries of the cyclacene with and without a knot, namely, Möbius and normal cyclacene, is very different from that based on the linear, prolate, and compact geometries of semiconductor clusters. Therefore, more different shape-dependences could be considered for semiconductor clusters in the future. The composition-dependence of polarizabilities is only available for the heteratomic clusters and less known than the size- and shape-dependences for semiconductor clusters [5, 30]. Karamanis *et al.* [30] investigated the composition-dependent polarizabilities of open- and closed-shell  $\text{Ga}_m\text{As}_n$  clusters with  $m + n = 5$  and 6. They showed that for a given size (5 or 6) the polarizabilities of the  $\text{Ga}_m\text{As}_n$  clusters gradually increase with increasing the number of Ga atoms in cluster. This dependence implies that for the heteratomic clusters we can obtain a tunable polarizability by adjusting the composition in clusters.

On the basis of the size, shape, and composition of the clusters, we can *qualitatively* understand the size of the polarizabilities. Other qualitative factors, such as the binding energy and ionization potentials, are often merged to the discussions of the size-, shape-, and composition-dependence. On the other hand, the size of the polarizabilities can be *quantitatively*

understood on the basis of both the energy gap and the dipole moment of a cluster. The former is based on the following sum-over-states (SOS) expression obtained from the simple perturbation theory:

$$\alpha_{ii} = 2 \sum_{k,l} \frac{|\langle k | \mu_i | l \rangle|^2}{E_l - E_k},$$

where the matrix elements correspond to the transition dipole moment between occupied ( $l$ ) and unoccupied ( $k$ ) states, and  $E_l - E_k$  is the corresponding transition energy. The latter is a correction made in the polarizability in the high temperature or low field limit and based on the expression: [6]

$$\alpha_{eff} = \langle \alpha \rangle + \frac{\mu^2}{3kT},$$

where  $\alpha_{eff}$  is the effective measured polarizability,  $\langle \alpha \rangle$  is the average polarizability, and  $\mu$  is the static dipole moment of the cluster. Although we prefer quantitatively understanding the size of polarizability, theoretical studies have shown that the energy gap factor is not well available for quantitatively understanding the size of the polarizability for the Si clusters and the effective polarizability increases the discrepancy between theoretical and experimental polarizabilities [11]. It is worthwhile to note that the temperature is also an important factor influencing the size of polarizability [36]. The temperature mentioned here is not the factor in the  $\alpha_{eff}$  expression. The temperature-dependence of polarizabilities was obtained by calculating the polarizabilities along the recorded trajectories of the Born-Oppenheimer molecular dynamics simulation at different finite temperatures. For some sodium clusters [36], the discrepancy between theory and experiment was explained by considering the finite temperature effects.

Obviously, studies of the evolution of polarizability are very useful in the design of nanomaterials. Especially on the basis of the composition-dependence of polarizability which has been shown interest in for semiconductor clusters [5, 30], we have more choices to obtain different polarizabilities by adjusting the cluster composition. Meanwhile, the cluster size, shape, and composition are three most intuitive factors that influence the size of the polarizability, which factor should we first consider in designing a new system? In this work, we theoretically study the size-, shape-, and composition-dependent polarizabilities of the  $\text{Si}_m\text{C}_n$  ( $m, n = 1 - 4$ ) clusters and evaluate the significance of these three factors for determining the size of polarizability.

In Section 2, we provide the computational details. In Section 3, we discuss the size-, shape-, and composition-dependent polarizabilities of the  $\text{Si}_m\text{C}_n$  ( $m, n = 1 - 4$ ) clusters. Finally, we summarize our results in Section 4.

## 2. Computational Details

There are many researches on the geometry and electronic structure of small SiC clusters. Low-lying isomers of these clusters were theoretically or experimental determined. For the aim of our present work, we selected the lowest-lying isomers and some low-lying isomers with different shapes (*i.e.*, linear, prolate, and compact clusters) of the  $\text{Si}_m\text{C}_n$  ( $m, n = 1 - 4$ ) clusters on the basis of the literature [37 – 40]. The selected low-lying isomers are the lowest energy isomers for a given shape. For example, the linear  $\text{D}_{\infty h}$  structure is the lowest-lying isomer or ground-state structure of  $\text{Si}_2\text{C}_3$  while the  $\text{C}_{2v}$  prolate structure is the lowest energy isomer for the prolate  $\text{Si}_2\text{C}_3$

clusters [37]. Note that there have been some discrepancies between the results of theoretical and experimental studies on the ground-state structure of the SiC clusters (even small clusters). For instance, most theoretical and experimental studies [41 – 44] have revealed that SiC<sub>3</sub> has three stable isomers (two having four-membered rings (C<sub>2v</sub>, <sup>1</sup>A<sub>1</sub>) and one with a linear structure (C<sub>infv</sub>, <sup>3</sup>Σ)) and that the global minimum structure of SiC<sub>3</sub> is a C<sub>2v</sub> prolate with a transannular C–C bond. However, these results are still controversial because the linear structure was predicted to be the ground state structure on the basis of highly accurate coupled-cluster calculations [45]. For the Si<sub>2</sub>C cluster [37, 38], the C<sub>2v</sub> and D<sub>infh</sub> singlet structures compete for the ground-state structure that depends on the level of theory. All the selected clusters were reoptimized at the DFT/aug-cc-pVTZ level with the hybrid Becke3-Lee-Yang-Parr (B3LYP) functional. The vibrational frequencies were calculated to confirm that the final geometries are stable without an imaginary frequency. The final geometries and their electronic states, symmetries, cluster shape, binding energies (*E<sub>b</sub>*), and energy gaps (*E<sub>g</sub>*) between the HOMO and LUMO are shown in Fig. 1.

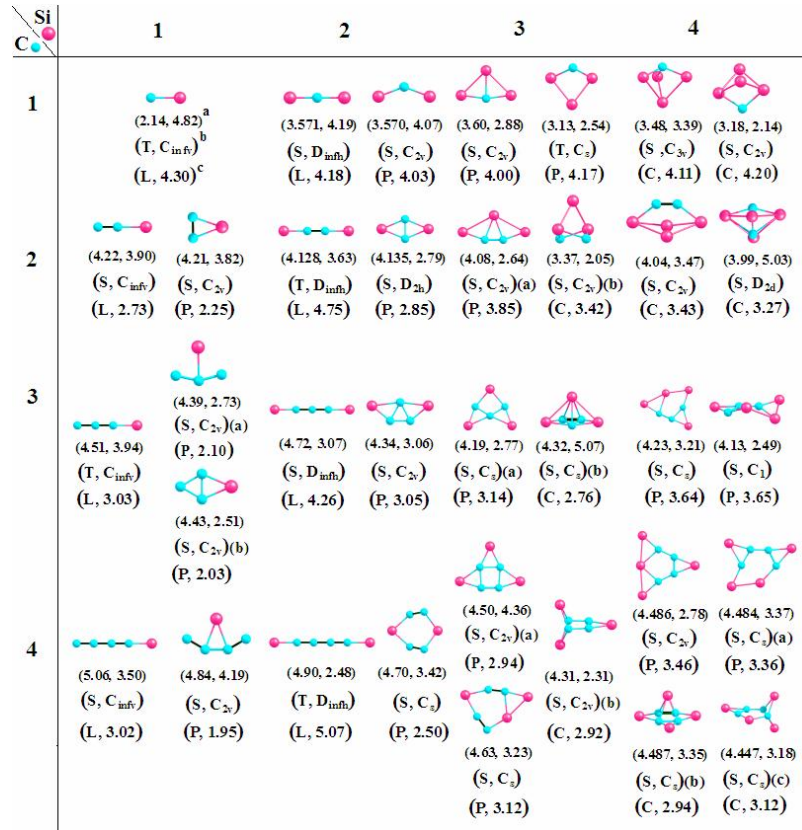


**Figure 1.** Geometries of the Si<sub>m</sub>C<sub>n</sub> (*m, n* = 1 – 4) clusters. <sup>a</sup> binding energy (in eV/atom) and energy gap (in eV). <sup>b</sup> electronic state and symmetry. <sup>c</sup> cluster shape and <*a*> (in Å<sup>3</sup>/atom). "L", "P", and "C" indicate the linear, prolate, and compact clusters, respectively.

For the estimation of the dipole polarizability (*α*), we focused on the isotropic dipole polarizability (<*α*>) which is defined as <*α*> = 1/3(*α<sub>xx</sub>* + *α<sub>yy</sub>* + *α<sub>zz</sub>*). The <*α*> is expressed in Å<sup>3</sup>/atom. Hereafter, *α* refers to <*α*>. To obtain reliable dipole polarizability, we should select an appropriate theoretic method and a reasonable basis set. In general, to obtain accurate *α* value, the diffuse and polarization functions and electron correlation effects should be considered in the calculation. For the density functional based methods, the local density approximation (LDA) and general gradient approximation (GGA) functionals can produce the close dipole polarizabilities.

For example, the Vosko-Wilk-Nusair (VWN), BLYP, and B3LYP functionals produce the polarizabilities of 5.17, 5.52, and 5.37 Å<sup>3</sup>/atom for the C<sub>2v</sub> singlet Si<sub>3</sub> cluster [13], respectively. Again, different hybrid functionals, such as the B3LYP, B3P86, and B3PW91 functionals, also produce very close polarizabilities [26, 20]. For the wave function based methods, the Møller-Plesset second order perturbation theory (MP2) with the aug-cc-pVDZ or the 6-31G augmented by the standard diffuse and polarization functions can lead to reliable dipole polarizabilities, which are very close to the results based on highly accurate coupled cluster singles-and-doubles (triplet) (CCSD(T)) calculations, for binary semiconductor clusters such as AlP and GaAs clusters [26 – 28, 30]. A more detailed discussion of the basis-set and theoretical method dependences of  $\alpha$  for small Si and SiC clusters can be found elsewhere [7, 13, 14, 19, 20]. In this work, we calculated the polarizabilities by using the coupled perturbed Hartree-Fock (CPHF) approach at the B3LYP/aug-cc-pVTZ level. A test B3LYP/aug-cc-pVTZ calculation performed on a CO molecule gave a polarizability of 1.95 Å<sup>3</sup> that is in good agreement with the experimental [46] and theoretical [47] values of 1.95 Å<sup>3</sup>. The calculated polarizabilities are also shown in Fig. 1. The polarizability of the SiC molecule was calculated by using both the CPHF and the finite field (FF) method at the aug-cc-pVTZ level for making a comparison with previous results [48] and also owing to no proper symmetry ( $\alpha_{xx}$ : 57.35,  $\alpha_{yy}$ : 34.46, and  $\alpha_{zz}$ : 59.54 a.u.) of three polarizability components based on the CPHF/B3LYP calculation. The FF/B3LYP and FF/MP2 method based on the fields of 0.003 (parallel) and 0.001 (perpendicular) a.u. give an isotropic polarizability of 4.40 and 3.84 Å<sup>3</sup>/atom, respectively. The FF/MP2//aug-cc-pVTZ result is in agreement with a polarizability of 3.86 Å<sup>3</sup>/atom based on the FF/MP2 with a self-designed basis set [48] and the fields of 0.003 (parallel) and 0.001 (perpendicular) a.u. The FF/B3LYP//aug-cc-pVTZ result was used for the SiC molecule in the following discussion. All the calculations were performed using the Gaussian 03 program [49].

### 3. Results and Discussion

#### 3.1 Size-dependence

We first investigate the size-dependent polarizabilities of the Si<sub>m</sub>C<sub>n</sub> ( $m, n = 1 - 4$ ) clusters. It can be expected that the size-dependence of the polarizabilities of heteroatomic clusters will be more complicated than that of homoatomic clusters because for a given cluster size the heteroatomic clusters have more isomers than the homoatomic ones. Figure 2a shows the size-dependent polarizabilities of the Si<sub>m</sub>C<sub>n</sub> ( $m, n = 1 - 4$ ) clusters. The cluster size is indicated by the number of atoms ( $N$ ) in cluster. For comparison, the polarizabilities based on the B3LYP calculations of the Si<sub>m</sub> ( $m = 1 - 8$ ) (Ref. [13, 20]), and C<sub>n</sub> (linear:  $n = 1 - 8$ ; cyclic:  $n = 4, 6$ , and 8) (Ref. [50]) clusters are included in Fig. 2a. The polarizabilities of the cyclic C<sub>n</sub> ( $n = 4, 6$ , and 8) clusters are 1.39, 1.44, and 1.50 Å<sup>3</sup>/atom, respectively. In Ref. [50], the  $\alpha$  values of the C<sub>n</sub> ( $n = 1 - 8$ ) clusters were calculated using a self-designed basis set that is different from the aug-cc-pVTZ we used here. Therefore, we recalculated the  $\alpha$  values of the C<sub>n</sub> ( $n = 1 - 8$ ) clusters to check the difference caused by the basis set effect. The obtained results are close to those of Ref. [50] and the difference is lower than ~0.03 Å<sup>3</sup>/atom. For example, we obtained a polarizability of 1.86 Å<sup>3</sup> for the C atom, which is close to 1.88 Å<sup>3</sup> reported in Ref. [50]. The Si, SiC, and C bulk values are also included in Fig. 2a and they are 3.71 (Ref. [6]), 1.84 (Ref. [19]), and 0.83 Å<sup>3</sup>/atom, respectively, which were obtained according to the Clausius-Mossotti relation. We calculated the C bulk value on the basis of the dielectric constant of 5.7 and the diamond density of 3.51 g/cm<sup>3</sup>.



To make a direct comparison with the  $\alpha$  values of the lowest-lying Si and C isomers, we plotted the size-dependent polarizabilities of the lowest-lying SiC isomers individually in Fig. 2a. As expected, small SiC clusters have a more complicated size-dependence of  $\alpha$  than small Si and C clusters. For small  $\text{Si}_m$  ( $m < 10$ ) clusters, the  $\alpha$  values are higher than the corresponding bulk value and decrease with an increase of the cluster size [5, 6, 13, 20, 50]. For small linear  $\text{C}_n$  ( $n \leq 8$ ,  $n \neq 2$ ) clusters, we can observe an increasing trend with an increase of the cluster size, which is attributed to an increasing trend of longitudinal component of  $\alpha$ . For small SiC clusters, although the  $\alpha$  values of the lowest-lying isomers are considered individually, we cannot observe a simple trend as small Si and C clusters. As shown in Fig. 2a, the  $\alpha$  values of the  $\text{Si}_m\text{C}_n$  ( $m, n = 1 - 4$ ) clusters are higher than the corresponding bulk value and have an oscillating variation with the cluster size.

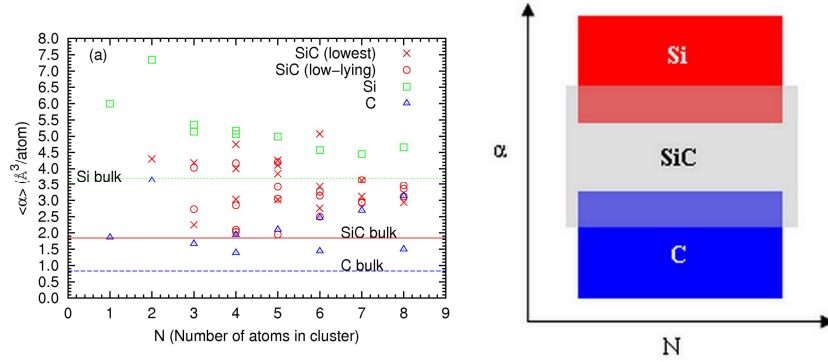


**Figure 2.** (a) Polarizabilities versus the cluster size ( $N$ ) for the  $\text{Si}_m\text{C}_n$  ( $m, n = 1 - 4$ ),  $\text{Si}_m$  ( $m = 1 - 8$ ), and  $\text{C}_n$  (linear:  $n = 1 - 8$ , cyclic:  $n = 4, 6$ , and  $8$ ) clusters. Dot line: Si bulk, Solid line: SiC bulk, Dash line: C bulk; (b) Size-distribution of  $\langle\alpha\rangle$  versus  $N$  for the  $\text{Si}_m\text{C}_n$  ( $m, n = 1 - 4$ ),  $\text{Si}_m$  ( $m = 1 - 8$ ), and  $\text{C}_n$  ( $n = 1 - 8$ ) clusters.

We can also see from Fig. 2a that the  $\alpha$  values of the SiC clusters lie between those of the Si and C clusters (*i.e.*, an order of  $\alpha(\text{Si}) > \alpha(\text{SiC}) > \alpha(\text{C})$ ), especially when the cluster size is fixed. For example, for diatomic clusters,  $\text{Si}_2$ ,  $\text{SiC}$ , and  $\text{C}_2$  clusters, their polarizabilities are 7.35, 4.30, and 3.63  $\text{\AA}^3/\text{atom}$ , respectively. The same case occurs for triatomic clusters. For some given cluster sizes, this order does not hold and the SiC cluster has a larger  $\alpha$  than the Si cluster or a smaller  $\alpha$  than the C cluster. For clarity, we show in Fig. 2b the size-distribution of  $\alpha$  versus  $N$  for the  $\text{Si}_m\text{C}_n$  ( $m, n = 1 - 4$ ),  $\text{Si}_m$  ( $m = 1 - 8$ ), and  $\text{C}_n$  (linear:  $n = 1 - 8$ ; cyclic:  $n = 4, 6$ , and  $8$ ) clusters. The two overlap regions in Fig. 2b indicate the order does not hold. For instance, for  $n = 6$ , the linear  $\text{Si}_2\text{C}_4$  cluster has a larger  $\alpha$  of 5.07  $\text{\AA}^3/\text{atom}$  (Fig. 1) than the compact  $\text{Si}_6$  cluster with 4.56  $\text{\AA}^3/\text{atom}$ . And for  $n = 8$ , the linear  $\text{C}_8$  cluster has a larger  $\alpha$  of 3.13  $\text{\AA}^3/\text{atom}$  than the prolate  $\text{C}_8$ (b)  $\text{Si}_4\text{C}_4$  cluster with 2.94  $\text{\AA}^3/\text{atom}$  (Fig. 1). These exceptions exist because for these clusters the shape effect (*i.e.*, linear  $\pi$  delocalized structure) significantly determines the size of  $\alpha$  (see discussion below). For  $N > 10$ , a comparison can not be made because of lack of the polarizabilities of the SiC and C clusters.

To understand the size of  $\alpha$  of the clusters, we first consider the approach based on the energy gap mentioned above. In the SOS expression, if we assume that the transitions between the HOMO and the LUMO make a major contribution to the polarizability, then the  $\alpha$  can be inversely related to the  $E_g$  (Refs. [6, 12, 13]). However, the inverse relationship between  $\alpha$  and  $E_g$  does not

hold in general because for some clusters the transition matrix element between the HOMO and the LUMO vanishes. For the  $\text{Si}_m$  ( $m < 30$ ) clusters, theoretical researches have shown that the correlation between  $\alpha$  and  $E_g$  is very weak [9, 11, 12]. For example, for the  $\text{Si}_m$  ( $m = 11-28$ ) clusters, the overall distribution in the plot of  $\alpha$  versus  $E_g$  is very scattered [11]. And for small  $\text{Si}_m$  ( $m = 3-10$ ) clusters, Pouchan *et al.* [13] used the density functional theory to show a direct correlation between the  $\alpha$  and the lowest symmetry-allowed transition energy gap not the energy gap, which is also understood on the basis of the SOS expression above. However, a research on the germanium clusters with 2 – 25 atoms [51] have shown a well correlation between  $\alpha$  and  $E_g$ , that is, the size of  $\alpha$  is inversely related to the size of  $E_g$  and a molecule with a smaller  $E_g$  is found to be softer and has a larger  $\alpha$ . In Fig. 3, we plot the  $\alpha$  values versus the  $E_g$  values for the  $\text{Si}_m\text{C}_n$  ( $m, n = 1-4$ ) clusters. The results also reveal an irregular correlation between  $\alpha$  and  $E_g$ .

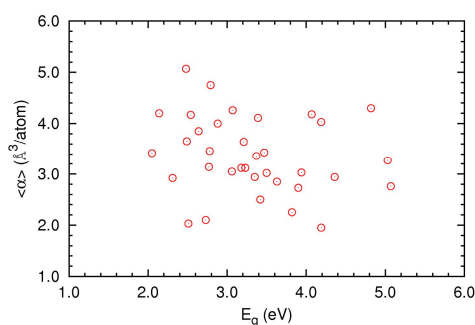


Figure 3. Polarizabilities versus the  $E_g$  values for the  $\text{Si}_m\text{C}_n$  ( $m, n = 1 - 4$ ) clusters.

On the other hand, one correlates the size of  $\alpha$  with  $E_g$  on the basis of the inverse relationship between  $\alpha$  and hardness. A harder molecule [52] has a larger  $E_g$ , in other words, a stable system with a large  $E_g$  (Ref. [1]) has a low polarizability according to the minimum polarizability principle [53 – 55] which points out that “the natural direction of evolution of any system is towards a state of minimum polarizability”. Note that the stability of a system can be also related to its  $E_b$  value [1], that is, a stable system has a large  $E_b$ . Therefore, we secondly attempt to correlate  $\alpha$  with  $E_b$ . Figure 4 shows the plots of  $\alpha$  versus  $E_b$  for the  $\text{Si}_m\text{C}_n$  ( $m, n = 1 - 4$ ) clusters. Similar to the  $E_g$ , the  $\alpha$  values have an irregular variation with the  $E_b$  values and the overall distribution is scattered.

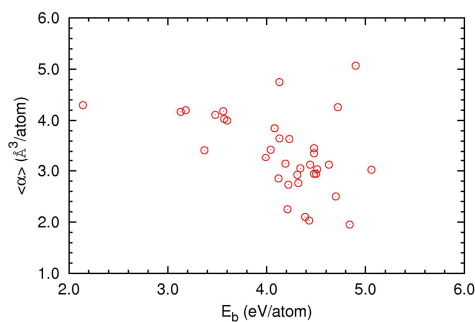
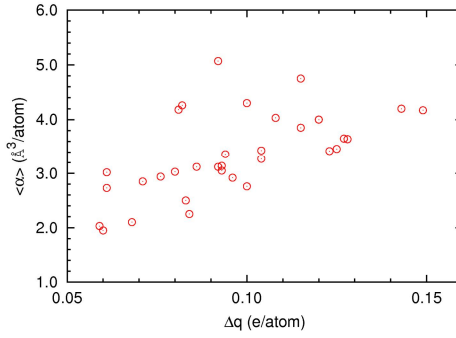


Figure 4. Polarizabilities versus the  $E_b$  values for the  $\text{Si}_m\text{C}_n$  ( $m, n = 1 - 4$ ) clusters.

Thirdly, we correlate the size of  $\alpha$  with the changes of the charge distribution related to an external field. Jackson *et al.* [9] used this approach to reveal that the response of the compact and prolate  $\text{Si}_m$  ( $m = 20 - 28$ ) clusters to a static external field is metallic on the basis of the metallic-like distribution of charge in these clusters. Karamanis *et al.* [26] employed this approach to show that the bonding effect is more important than the cluster composition on the hyperpolarizability values for a series of  $\text{Al}_n\text{P}_n$  ( $n = 2, 3, 4, 6$ , and 9) clusters. The response of a molecule to an external field leads to a redistribution of atomic charge in cluster, especially for the surface atoms [9]. In our present work, we use a parameter:

$$\Delta q = \frac{1}{3N} \sum_j \Delta q_j = \frac{1}{3N} \sum_j \sum_i |q_i(F_j) - q_i(0)|$$

to characterize the redistribution of charge, where  $N$  is the cluster size,  $q_i(F_j)$  is the natural charge of atom  $i$  perturbed by a  $F_j$  external field in the direction  $j = x, y, z$ , and  $q_i(0)$  is the natural charge of an unperturbed molecule. A field of 0.02 a.u. was applied to calculate the natural charge. We collected the calculated results in Table 1 where three polarizability components ( $\alpha_{xx}$ ,  $\alpha_{yy}$ , and  $\alpha_{zz}$ ) are also included. From Table 1, we observe the same size order for the components of  $\alpha$  and  $\Delta q$ . For example, the prolate  $\text{SiC}_2$  cluster has orders of  $\alpha_{xx} < \alpha_{yy} < \alpha_{zz}$  and  $\Delta q_x < \Delta q_y < \Delta q_z$ . We assume that the cluster with a larger  $\Delta q$  would have a larger polarizability because the electric polarization leads the charge distribution of a molecule to distort from its normal shape. Figure 5 shows the plots of  $\alpha$  versus  $\Delta q$  for the  $\text{Si}_m\text{C}_n$  ( $m, n = 1 - 4$ ) clusters. Compared with both  $E_g$  and  $E_b$ , the  $\alpha$  values have an overall increasing trend with an increase of the  $\Delta q$  values. The  $\Delta q$  is a good factor for understanding the size of  $\alpha$ . We will find better correlations between  $\alpha$  and both  $E_b$  and  $\Delta q$  than  $E_g$  provided that both the cluster shape and one of the components in cluster are fixed (see discussion below).



**Figure 5.** Polarizabilities versus the  $\Delta q$  values for the  $\text{Si}_m\text{C}_n$  ( $m, n = 1 - 4$ ) clusters.

**Table 1.**  $\Delta q_x$ ,  $\alpha_{xx}$ ,  $\Delta q_y$ ,  $\alpha_{yy}$ ,  $\Delta q_z$ ,  $\alpha_{zz}$ , and  $\Delta q$  of the  $\text{Si}_m\text{C}_n$  ( $m, n = 1 - 4$ ) clusters. "L", "P", and "C" indicate the linear, prolate, and compact clusters, respectively. <sup>a</sup> cluster shape and symmetry.

Cluster	$\Delta q_x$ (e)	$\alpha_{xx}$ ( $\text{\AA}^3$ )	$\Delta q_y$ (e)	$\alpha_{yy}$ ( $\text{\AA}^3$ )	$\Delta q_z$ (e)	$\alpha_{zz}$ ( $\text{\AA}^3$ )	$\Delta q$ (e/atom)
$\text{SiC}$ (L, $\text{C}_{\text{infv}}$ ) <sup>a</sup>	0.017	8.48	0.017	8.48	0.563	8.82	0.100
$\text{SiC}_2$ (P, $\text{C}_{2v}$ )	0.017	5.49	0.286	6.87	0.452	7.90	0.084
$\text{SiC}_2$ (L, $\text{C}_{\text{infv}}$ )	0.003	6.23	0.003	6.23	0.545	12.14	0.061
$\text{SiC}_3$ (P, $\text{C}_{2v}$ ) (a)	0.013	6.47	0.367	7.39	0.441	10.55	0.068
$\text{SiC}_3$ (P, $\text{C}_{2v}$ ) (b)	0.009	6.53	0.238	9.56	0.466	9.15	0.059
$\text{SiC}_3$ (L, $\text{C}_{\text{infv}}$ )	0.013	7.21	0.013	7.21	0.932	21.95	0.080



SiC <sub>4</sub> (P, C <sub>2v</sub> )	0.005	6.72	0.542	13.20	0.359	9.34	0.060
SiC <sub>4</sub> (L, C <sub>infv</sub> )	0.011	7.79	0.011	7.79	0.895	29.69	0.061
Si <sub>2</sub> C (P, C <sub>2v</sub> )	0.000	9.02	0.709	18.24	0.263	9.05	0.108
Si <sub>2</sub> C (L, D <sub>infh</sub> )	0.003	9.26	0.003	9.27	0.722	19.10	0.081
Si <sub>2</sub> C <sub>2</sub> (P, D <sub>2h</sub> )	0.011	8.55	0.244	9.09	0.597	16.57	0.071
Si <sub>2</sub> C <sub>2</sub> (L, D <sub>infh</sub> )	0.023	10.13	0.023	10.13	1.330	36.69	0.115
Si <sub>2</sub> C <sub>3</sub> (P, C <sub>2v</sub> )	0.009	9.78	0.925	25.43	0.467	10.53	0.093
Si <sub>2</sub> C <sub>3</sub> (L, D <sub>infh</sub> )	0.011	10.59	0.011	10.59	1.201	42.65	0.082
Si <sub>2</sub> C <sub>4</sub> (L, D <sub>infh</sub> )	0.006	11.73	0.006	11.73	1.641	67.88	0.092
Si <sub>2</sub> C <sub>4</sub> (P, C <sub>s</sub> )	0.422	12.08	0.755	19.25	0.319	13.74	0.083
Si <sub>3</sub> C (P, C <sub>2v</sub> )	0.002	11.06	0.761	21.66	0.677	15.27	0.120
Si <sub>3</sub> C (P, C <sub>s</sub> )	0.276	11.95	0.789	17.59	0.719	20.52	0.149
Si <sub>3</sub> C <sub>2</sub> (P, C <sub>2v</sub> ) (a)	0.036	12.12	1.267	31.64	0.417	13.96	0.115
Si <sub>3</sub> C <sub>2</sub> (C, C <sub>2v</sub> ) (b)	0.371	14.07	0.618	19.27	0.851	17.98	0.123
Si <sub>3</sub> C <sub>3</sub> (P, C <sub>s</sub> ) (a)	0.192	15.52	0.842	13.10	0.641	21.09	0.093
Si <sub>3</sub> C <sub>3</sub> (C, C <sub>s</sub> ) (b)	0.636	12.78	0.470	20.76	0.692	22.96	0.100
Si <sub>3</sub> C <sub>4</sub> (P, C <sub>2v</sub> ) (a)	0.008	21.21	0.874	13.63	0.706	26.50	0.076
Si <sub>3</sub> C <sub>4</sub> (C, C <sub>2v</sub> ) (b)	0.714	32.91	0.317	19.52	0.989	13.07	0.096
Si <sub>3</sub> C <sub>4</sub> (P, C <sub>s</sub> )	0.992	12.63	0.758	28.17	0.050	21.04	0.086
Si <sub>4</sub> C (C, C <sub>2v</sub> )	0.813	23.56	0.621	21.35	0.715	18.02	0.143
Si <sub>4</sub> C (C, C <sub>3v</sub> )	0.923	21.61	0.880	21.61	0.707	18.43	0.167
Si <sub>4</sub> C <sub>2</sub> (C, C <sub>2v</sub> )	0.650	20.23	0.803	26.42	0.417	15.17	0.104
Si <sub>4</sub> C <sub>2</sub> (C, D <sub>2d</sub> )	0.714	22.21	0.714	22.21	0.438	14.47	0.104
Si <sub>4</sub> C <sub>3</sub> (P, C <sub>1</sub> )	1.184	33.66	1.010	26.44	0.466	16.57	0.127
Si <sub>4</sub> C <sub>3</sub> (P, C <sub>s</sub> )	0.929	26.12	1.292	35.21	0.466	15.16	0.128
Si <sub>4</sub> C <sub>4</sub> (P, C <sub>2v</sub> )	0.023	15.85	1.298	34.49	1.683	32.76	0.125
Si <sub>4</sub> C <sub>4</sub> (P, C <sub>s</sub> ) (a)	0.924	28.70	1.310	35.99	0.026	15.95	0.094
Si <sub>4</sub> C <sub>4</sub> (C, C <sub>s</sub> ) (b)	0.430	18.48	0.706	25.80	0.699	26.27	0.076
Si <sub>4</sub> C <sub>4</sub> (C, C <sub>s</sub> ) (c)	0.722	22.18	0.924	30.16	0.574	22.49	0.092

### 3.2 Shape-dependence

It is well known that organic molecules with a linear or prolate geometry have a large (hyper)polarizability because they have a delocalized  $\pi$ -conjugated structure [33, 56]. Constructing a  $\pi$ -conjugated structure has become one of choices to design a new molecule with large (hyper)polarizability [57]. For small SiC clusters with increasing the cluster size, three alternative hybridizations ( $sp$ ,  $sp^2$ , and  $sp^3$ ) of C atom result in a variation from linear to prolate, then compact structure in lowest-lying isomers while the  $sp^3$  hybridization of Si atom leads to a variation from prolate to compact structure. A transition from prolate to compact will lead to a decrease of the electron delocalization, ultimately, a decrease of the (hyper)polarizability [26, 28]. Experimental and theoretical studies have provided sufficient information on the geometry [3, 37,

[38, 58 – 62] for the  $\text{Si}_m\text{C}_n$  ( $n + m < 8$ ) clusters. The structure of the  $\text{SiC}$  cluster is a result of the competition for bonding that occurs between the C and the Si atoms. As shown in Fig. 1, C-rich clusters tend to exist in the linear or prolate structure while Si-rich clusters prefer forming prolate or compact structure. For example, the lowest-lying isomers of the  $\text{SiC}_n$  ( $n = 2, 3$ , and 4) clusters are the linear structure while those of the  $\text{Si}_m\text{C}$  ( $m = 2, 3$ , and 4) clusters are prolate or compact structure (Fig. 1). In our recent work [19], we have shown that the size-dependence of the first-order hyperpolarizabilities of the  $\text{SiC}_n$  ( $n = 2 - 6$ ) clusters, which have approximate Si-terminated linear chain geometry, is similar to that observed in  $\pi$ -conjugated organic molecules. For semiconductor clusters such as Si, AlP, and GaAs clusters, theoretical researches have shown that the prolate clusters have systematically larger polarizabilities than the compact ones [9, 11, 12, 26, 27, 31, 32]. Therefore, the size of the (hyper)polarizability, to some degree, depends on the geometry or shape of a cluster.

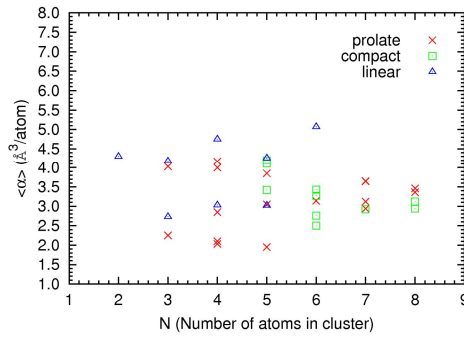
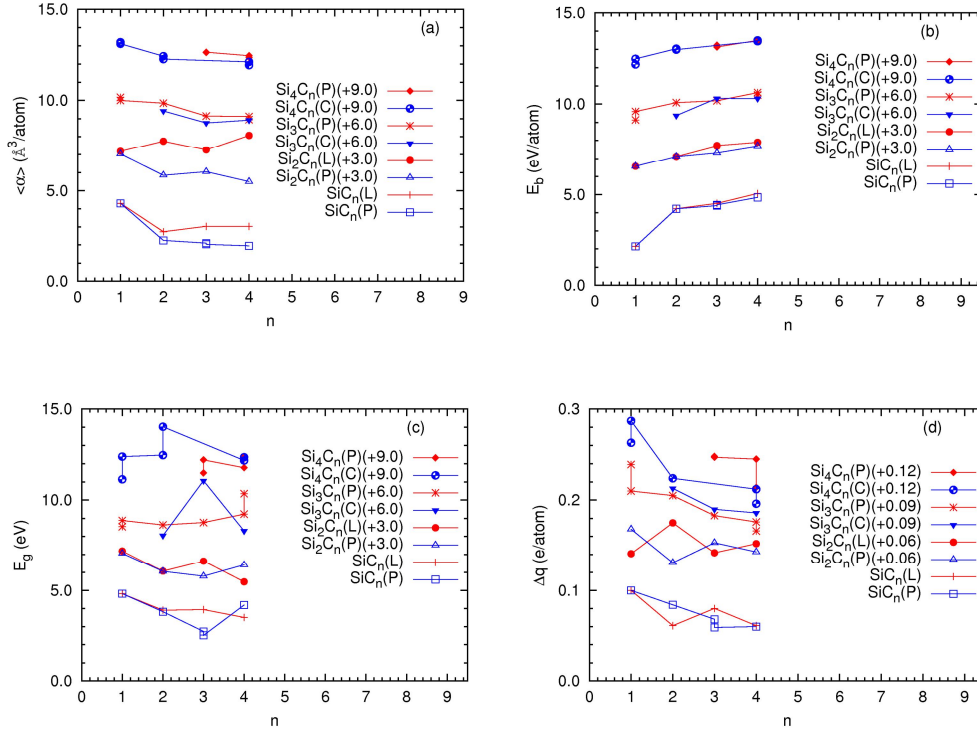


Figure 6. Shape dependence of the  $\langle\alpha\rangle$  values for the  $\text{Si}_m\text{C}_n$  ( $m, n = 1 - 4$ ) clusters.

Figure 6 shows the shape-dependence of  $\alpha$  for the  $\text{Si}_m\text{C}_n$  ( $m, n = 1 - 4$ ) clusters. Although no clear correlation is observed between the size of  $\alpha$  and the cluster shape from Fig. 6, we can see that most of the linear clusters have a large  $\alpha$  and the shape-dependence of  $\alpha$  will be clear when the cluster size and composition are fixed. For example, for triatomic clusters ( $\text{Si}_2\text{C}$  and  $\text{SiC}_2$ ), the linear and prolate  $\text{Si}_2\text{C}$  clusters have the  $\alpha$  values of 4.18 and 4.03  $\text{\AA}^3/\text{atom}$ , respectively, and for the linear and prolate  $\text{SiC}_2$  clusters they are 2.73 and 2.25  $\text{\AA}^3/\text{atom}$ , respectively (Fig. 1). A similar case occurs for tetra-atomic clusters ( $\text{Si}_2\text{C}_2$  and  $\text{SiC}_3$  clusters). In detail, Fig. 7a shows the plots of the  $\alpha$  values versus the number of C atoms ( $n$ ) in cluster with both the cluster shape and the number of Si atoms fixed. From Fig. 7a, we can clearly observe orders of  $\alpha(\text{L}) > \alpha(\text{P})$  and  $\alpha(\text{P}) > \alpha(\text{C})$  for a given composition. For the prolate and compact series clusters, the  $\alpha$  values decrease with an increase of the number of C atoms ( $n$ ) in cluster, which indicates a composition-dependence of  $\alpha$  (see discussion below).



**Figure 7.** (a) Polarizabilities, (b) Binding energies, (c) Energy gaps, and (d)  $\Delta q$  versus the number of C atoms ( $n$ ) in cluster with both the cluster shape and the number of Si atoms fixed. (L), (P), and (C) indicate the linear, prolate, and compact clusters, respectively. (+3.0) indicates 3.0 is added to the  $\langle\alpha\rangle$  values to clearly display the plots. Other factors have a similar meaning.

To understand the shape-dependence of  $\alpha$  for the  $\text{Si}_m\text{C}_n$  ( $m, n = 1 - 4$ ) clusters, we attempt to use the following approaches:

(1) Using both  $E_g$  and  $E_b$ . As mentioned above, both  $E_g$  and  $E_b$  have no regular overall variation with the size of  $\alpha$ . In Figs. 7b and 7c, we plot the  $E_b$  and the  $E_g$  versus the number of C atoms ( $n$ ) in cluster, respectively, corresponding to the clusters considered in Fig. 7a. On the basis of the SOS expression, we would have a larger  $\alpha$  for the cluster with a smaller  $E_g$ , but in Fig. 7c this behavior has not been observed for all clusters except  $\text{SiC}_4$  (L and P) and  $\text{Si}_3\text{C}_3$  (P and C). Therefore, the shape dependence cannot be explained by the  $E_g$  even when both the cluster size and the cluster shape are fixed, in accord with the Jackson *et al.* [9] who had shown that the differences between the  $\alpha$  values of the prolate and compact clusters cannot be explained on the basis of the  $E_g$  for the  $\text{Si}_m$  ( $m = 20-28$ ) clusters. For the  $E_b$ , similar to the  $E_g$ , no obvious correlation with the cluster shape was observed, however, for all series of clusters except  $\text{Si}_2\text{C}_n$  (L) we can observe an inverse relationship between  $\alpha$  and  $E_b$ , in agreement with the fact that a cluster has a high stability and a low polarizability.

(2) Using a geometrical parameter,

$$I = \sum_{i=1}^n r_i^2,$$

where  $r_i$  is the distance of atom  $i$  to the cluster center of mass and  $n$  is the number of atoms in cluster. Deng *et al.* [11] used this approach to explain the evolution of  $\alpha$  for the  $\text{Si}_m$  ( $m = 9 - 28$ )

clusters and showed that more elongated clusters are more polarizable. However, Jackson *et al.* [9] found that the shape-dependence of the *total* polarizabilities is clearly more complicated than the difference in  $I$  between the compact and the prolate  $\text{Si}_m$  ( $m = 20\text{--}28$ ) clusters. For the SiC clusters we considered here, the  $I$  values are close between different shape clusters especially for a given cluster size because the clusters have small size ( $N \leq 8$ ). Therefore, this approach is not available for us.

(3) Using the  $\Delta q$  defined above. In Fig. 7d, we plot the  $\Delta q$  versus the number of C atoms ( $n$ ), corresponding to the clusters considered in Fig. 7a. Combining with Fig. 7a, we can see that the shape dependence of  $\alpha$  cannot be reflected by the size of the  $\Delta q$ . For example, for the linear and prolate  $\text{Si}_2\text{C}_n$  clusters with a given  $n$ , the linear  $\text{Si}_2\text{C}_n$  cluster has a larger  $\alpha$  than the compact  $\text{Si}_2\text{C}_n$  one (Fig. 7a) while the size orders of  $\Delta q$  between prolate and compact clusters alternately change with increasing the number of C atoms ( $n$ ) (Fig. 7d). And for the prolate and compact  $\text{Si}_3\text{C}_n$  clusters with a given  $n$ , reverse size orders are observed for the  $\alpha$  and  $\Delta q$  values. However, it is interesting that the  $\alpha$  values have the same variation trend as the  $\Delta q$  with an increase of the number of C atoms for each series of clusters. Comparing Fig. 7d with Fig. 7b, we can see that the  $\Delta q$  is more available than the  $E_b$  for qualitatively understanding the size of  $\alpha$ . For instance, for both the linear and the prolate  $\text{Si}_2\text{C}_n$  clusters, the  $\Delta q$  values can well reflect the evolutions of  $\alpha$  (Fig. 7a and Fig. 7d) while the  $E_b$  values cannot (Fig. 7a and Fig. 7b). Furthermore, some isomers with very close  $E_b$  values and different  $\alpha$  values may be identified by the  $\Delta q$  values. For example, for the  $\text{Si}_4\text{C}_4(\text{C}_{2v})$ ,  $\text{Si}_4\text{C}_4(\text{C}_s(\text{a}))$ , and  $\text{Si}_4\text{C}_4(\text{C}_s(\text{b}))$  clusters whose  $E_b$  values are 4.486, 4.484, and 4.487 eV/atom (Fig. 1), respectively, the size of  $\alpha$  ( $\text{Si}_4\text{C}_4(\text{C}_{2v})$ :  $3.46 \text{ \AA}^3/\text{atom}$ ,  $\text{Si}_4\text{C}_4(\text{C}_s(\text{a}))$ :  $3.36 \text{ \AA}^3/\text{atom}$ ,  $\text{Si}_4\text{C}_4(\text{C}_s(\text{b}))$ :  $2.94 \text{ \AA}^3/\text{atom}$ ) is well related to that of  $\Delta q$  ( $\text{Si}_4\text{C}_4(\text{C}_{2v})$ : 0.125 e/atom,  $\text{Si}_4\text{C}_4(\text{C}_s(\text{a}))$ : 0.094 e/atom, and  $\text{Si}_4\text{C}_4(\text{C}_s(\text{b}))$ : 0.076 e/atom, respectively).

(4) Considering the delocalization of  $\pi$ -electron structure. Organic molecules with  $\pi$ -electron delocalization have a large (hyper)polarizability [33, 56] because a  $\pi$ -electron delocalization leads to a strong charge separation. As shown in Fig. 1, both the linear and the prolate clusters would form a  $\pi$ -electron delocalization framework. Although the transition between the HOMO and the LUMO does not determine the size of  $\alpha$ , the transitions between different frontier MOs generally make significant contributions to the size of  $\alpha$  on the basis of the SOS expression [19]. To check the distribution of electron, we provide in Fig. 8 the HOMO–1, HOMO, LUMO, and LUMO+1 of the  $\text{SiC}_2$ ,  $\text{SiC}_4$ ,  $\text{Si}_3\text{C}_2$ ,  $\text{Si}_3\text{C}_3$ , and  $\text{Si}_4\text{C}_4$  clusters based on the B3LYP/aug-cc-pVTZ wave function. It is clearly shown that for a given cluster size, the linear cluster has more  $\pi$ -delocalized frontier molecular orbital (MO) than the prolate one. For example, the linear  $\text{SiC}_2$  cluster has four  $\pi$ -delocalized MOs (two-fold degenerate HOMO–1 and LUMO) while the prolate  $\text{SiC}_2$  cluster has only one  $\pi$ -delocalized MO (LUMO+1). Similarly, for the prolate and compact clusters, the prolate cluster has more obvious  $\pi$ -delocalized MO than the compact one. Therefore, the shape-dependence of  $\alpha$  can be understood on the basis of the electron delocalization of these frontier MOs.

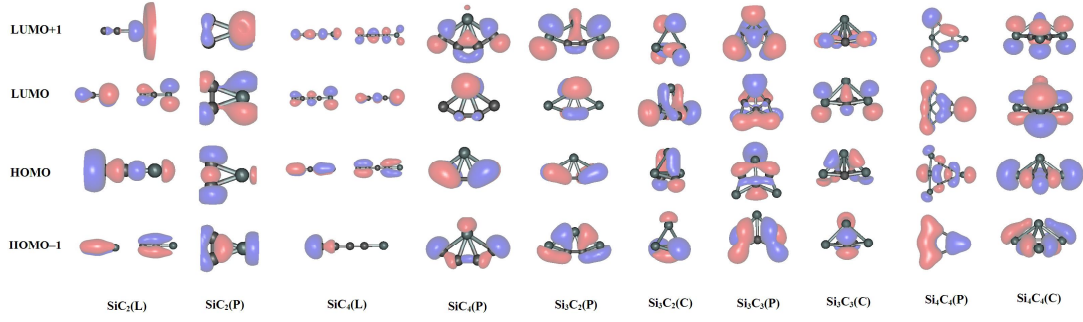


**Figure 8.** *HOMO-1, HOMO, LUMO, and LUMO+1 of  $\text{SiC}_2$ ,  $\text{SiC}_4$ ,  $\text{Si}_3\text{C}_2$ ,  $\text{Si}_3\text{C}_3$ , and  $\text{Si}_4\text{C}_4$  clusters.*

### 3.3 Composition-dependence

As mentioned above, for heteroatomic clusters such as AlP and GaAs clusters, the size of  $\alpha$  also strongly depends on the cluster composition [29, 30]. Figure 9 shows the plots of the  $\alpha$  values versus the  $m/n$  values for the  $\text{Si}_m\text{C}_n$  ( $m, n = 1 - 4$ ) clusters. Regardless of the cluster shape, we cannot observe a clear correlation between  $\alpha$  and  $m/n$  from Fig. 9. The linear clusters have an obvious larger polarizability than both the prolate and the compact clusters especially for a given  $m/n$  value. We notice that four linear clusters with small  $m/n$  ratio have a large  $\alpha$ . These four clusters are  $\text{SiC}$ ,  $\text{Si}_2\text{C}_4$ ,  $\text{Si}_2\text{C}_3$ , and  $\text{Si}_2\text{C}_2$  with 4.30, 5.07, 4.26, and 4.75  $\text{\AA}^3/\text{atom}$ , respectively. Combining with the shape-dependence of  $\alpha$ , we can conclude that the shape effect makes a main contribution to the size of  $\alpha$  for these four clusters because they have very different cluster sizes ( $N = 2, 6, 5$ , and 4, respectively) and small  $m/n$  ratios ( $\leq 1.0$ ). When excluding the linear clusters, we can observe an overall increasing trend of  $\alpha$  with an increase of  $m/n$ . A nonlinear fit for the  $\alpha$  values versus the  $m/n$  values of the prolate and compact clusters give an expression of  $\alpha = A - (A - B) \times \exp(-k(m/n))$ , where  $A = 4.3$ ,  $B = 1.5$ , and  $k = 0.87$ . The  $A$  and  $B$  values locate at the region of the  $\alpha$  values of pure Si and C clusters, respectively (Fig. 2a). This expression indicates that the  $\alpha$  values of small SiC clusters would tend towards those of pure  $\text{Si}_m$  clusters with  $n = 0$  and towards those of pure  $\text{C}_n$  clusters with  $m = 0$ . This dependence is very useful for us to design a SiC cluster with an expected  $\alpha$  value.

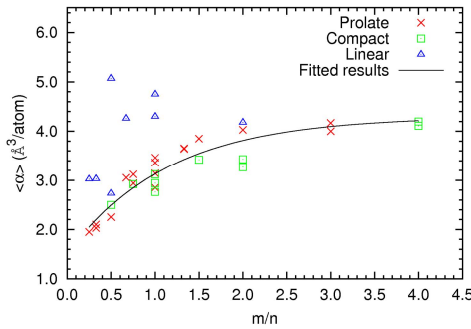


**Figure 9.** *Polarizabilities versus the cluster composition (i.e.,  $m/n$  ratio) for the  $\text{Si}_m\text{C}_n$  ( $m, n = 1 - 4$ ) clusters.*

Similar to the GaAs cluster [30], we can understand the composition-dependence of  $\alpha$  in

terms of the atomic polarizabilities of C and Si atoms. On the basis of the B3LYP/aug-cc-pVTZ calculations, we obtained the  $\alpha$  values of 1.86 and 6.00  $\text{\AA}^3$  for C and Si atoms, respectively. The  $\alpha$  value of Si atom is three times larger than that of C atom. As shown in the polarizabilities of GaAs clusters [30], a replacement of As by Ga in cluster will increase the polarizability because the  $\alpha$  of Ga atom is almost twice that of As atom. A same case occurs for the SiC cluster we considered here provided that the cluster shape is fixed. Actually, all the lowest-lying GaAs clusters considered by Karamanis *et al.* [30] have a compact structure except that the  $\text{Ga}_4\text{As}$  with a prolate structure has a largest  $\alpha$  among four pentaatomic GaAs clusters. In our present work, for  $N = 5$ , the compact  $\text{Si}_4\text{C}$  (4.11  $\text{\AA}^3/\text{atom}$ ), the prolate  $\text{Si}_3\text{C}_2$  (3.85  $\text{\AA}^3/\text{atom}$ ), and the linear  $\text{Si}_2\text{C}_3$  (4.26  $\text{\AA}^3/\text{atom}$ ) clusters individually have a larger  $\alpha$  than the compact  $\text{Si}_3\text{C}_2$  (3.42  $\text{\AA}^3/\text{atom}$ ), the prolate  $\text{Si}_2\text{C}_3$  (3.05  $\text{\AA}^3/\text{atom}$ ), and the linear  $\text{SiC}_4$  (3.02  $\text{\AA}^3/\text{atom}$ ) clusters. Note that the linear  $\text{Si}_2\text{C}_3$  cluster has a largest  $\alpha$ , which implies that the shape effect makes a main contribution to determining the size of  $\alpha$ .

From Fig. 7a, we have seen that the  $\alpha$  values decrease with an increase of the number of C atoms ( $n$ ) when both the cluster shape and the number of Si atoms in clusters are fixed. Furthermore, in Fig. 10, we plot the  $\alpha$  values versus the number of Si atoms ( $m$ ) with both the cluster shape and the number of C atoms fixed. All the clusters considered in Fig. 10 have a prolate structure. Interestingly, we find that the  $\alpha$  values increase with an increase of the number of Si atoms ( $m$ ). In Fig. 10, we also include the plots of the  $E_b$ , the  $E_g$ , and the  $\Delta q$  versus the  $m$  to further check the correlation between  $\alpha$  and  $E_b$ ,  $E_g$ , and  $\Delta q$ , respectively. As shown in Fig. 10, both the  $E_b$  and the  $\Delta q$  are more available than the  $E_g$  for understanding the size of  $\alpha$ , in agreement with the discussion above.

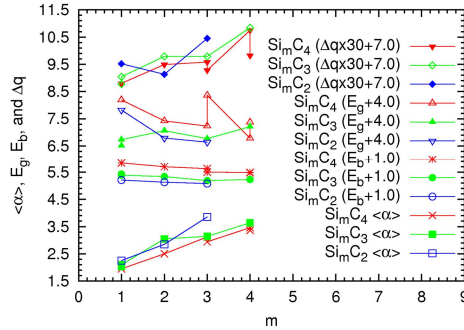


Figure 10. Polarizabilities ( $\text{\AA}^3/\text{atom}$ ),  $E_b$  (eV/atom),  $E_g$  (eV), and  $\Delta q$  (e/atom) versus the number of Si atoms ( $m$ ) in cluster with the number of C atoms fixed. (+1.0) indicates 1.0 is added to the  $E_b$  values to clearly display the plots. Other factors have a similar meaning.

#### 4. Conclusions

In this study, we have theoretically investigated the size-, shape-, and composition-dependent polarizabilities of the  $\text{Si}_m\text{C}_n$  ( $m, n = 1 - 4$ ) clusters. On the basis of the size- (Fig. 2a), shape- (Fig. 6), and composition- (Fig. 9) dependence of  $\alpha$ , we should first consider the shape effect to design a new cluster with a large polarizability. Note that Fig. 6 also reflects the size-dependence of  $\alpha$  of the  $\text{Si}_m\text{C}_n$  ( $m, n = 1 - 4$ ) clusters. For small clusters up to about 8 atoms, on the basis of the bonding feature of the atoms and the compositions of atoms in cluster, we first consider linear or



prolate cluster. For example, for the  $\text{SiC}_n$  clusters, we first consider the linear clusters as the C atoms are main components in these clusters and have three alternative hybridizations of  $sp$ ,  $sp^2$ , and  $sp^3$ . And for the  $\text{Si}_3\text{C}_n$  ( $n < 4$ ) clusters, we first consider the prolate clusters as the Si atoms are main components in these clusters and prefer the  $sp^3$  hybridization. Furthermore, since it is difficult for most atoms to form a linear structure, the prolate clusters should be first considered as a cluster with a large polarizability. For example, the prolate  $\text{Si}_3$  ( $\text{C}_{2v}$ ),  $\text{Si}_4$  ( $\text{D}_{2h}$ ),  $\text{Al}_2\text{P}_2$  ( $\text{D}_{2h}$ ),  $\text{Al}_3\text{P}_3$  ( $\text{D}_{3h}$ ),  $\text{Ga}_2\text{As}_2$  ( $\text{D}_{2h}$ ), and  $\text{Ga}_4\text{As}$  ( $\text{C}_{2v}$ ) clusters have a large polarizability per atom [6, 7, 13, 20, 28, 30]. For mediate-size clusters, we first consider the prolate clusters, in accordance with the evolution of the calculated polarizabilities of the artificial *prolate*  $(\text{Al}_4\text{P}_4)_N$  ( $N = 2 - 6$ ),  $(\text{Al}_3\text{P}_3)_N$  ( $N = 3 - 8$ ), and  $(\text{GaAs})_N$  ( $N = 10, 14, 18, 22$ , and  $26$ ) clusters [27, 32].

Meanwhile, after Karamanis *et al.* and Jackson *et al.* [9, 26, 27,], we further demonstrate that the redistribution of charge caused by an applied external field is a good factor to qualitatively understand the size of polarizability. Although both the  $E_g$  and the  $E_b$  are generally used to characterize the stability of a cluster, the  $E_b$  is more available than the  $E_g$  for reflecting the size of polarizability. For the isomers with very close energy, the  $E_b$  can not reflect the size of polarizability while the  $\Delta q$  can do well in.

### Acknowledgement

The authors are grateful for the financial support provided by the Foundation of Zhejiang Key Laboratory for Reactive Chemistry on Solid Surfaces.

### References

- [1] H.S. Nalwa, *Handbook of Thin Films Materials*, Volume 5: Nanomaterials and Magnetic Thin Films. Academic Press, New York, and 2002, Chapter 2.
- [2] Y. Kawazoe, T. Kondow, and K. Ohno, *Clusters and Nanomaterials* (Springer Series in Cluster Physics). Springer-Verlag Berlin and Heidelberg GmbH & Co. K, 2002.
- [3] M. Bertolus, V. Brenner, and P. Milli , Eur. Phys. J. D **1**, 197 (1998).
- [4] I. Vasiliev, S.  g t and J. R. Chelikowsky, Phys. Rev. B **60**, R8477 (1999).
- [5] R. Sch fer, S. Schlecht, J. Woenckhaus, and J. A. Becker, Phys. Rev. Lett. **76**, 471 (1996).
- [6] I. Vasiliev, S.  g t, and J. R. Chelikowsky, Phys. Rev. Lett. **78**, 4805 (1997).
- [7] V. E. Bazterra, M. C. Caputo, M. B. Ferraro and P. Fuentealba, J. Chem. Phys. **117**, 11158 (2002).
- [8] G. Maroulis and C. Pouchan, J. Phys. B: At. Mol. Opt. Phys. **36**, 2011 (2003).
- [9] K. A. Jackson, M. Yang, I. Chaudhuri, and Th. Frauenheim, Phys. Rev. A **71**, 033205 (2005).
- [10] Y. Mochizuki and H.  gren, Chem. Phys. Lett. **336**, 451 (2001).
- [11] K. Deng, J. L. Yang, and C. T. Chan, Phys. Rev. A **61**, 025201 (2000).
- [12] K. Jackson, M. Pederson, C. Z. Wang, and K. M. Ho, Phys. Rev. A **59**, 3685 (1999).
- [13] C. Pouchan, D. B gu , and D. Y. Zhang, J. Chem. Phys. **121**, 4628 (2004).
- [14] G. Maroulis, D. B gu , and C. Pouchan, J. Chem. Phys. **119**, 794 (2003).
- [15] G. Maroulis and C. Pouchan, Phys. Chem. Chem. Phys. **5**, 1992 (2003).
- [16] D. B gu , C. Pouchan, G. Maroulis, and D. Y. Zhang, J. Comp. Meth. Sci. Eng. **6**, 223 (2006).
- [17] T. T. Rantala and M. I. Stockman, D. A. Jelski, and T. F. George, J. Chem. Phys. **93**, 7427 (1990).
- [18] Y. Z. Lan, Y. L. Feng, Y. H. Wen, and B. T. Teng, Chem. Phys. Lett. **461**, 118 (2008).

- [19] Y. Z. Lan and Y. L. Feng, J. Chem. Phys. **131**, 054509 (2009).
- [20] Y. Z. Lan, Y. L. Feng, Y. H. Wen and B. T. Teng, J. Mol. Struct. (Theochem) **854**, 63 (2008).
- [21] Y. Z. Lan, W. D. Cheng, D. S. Wu, J. Shen, S. P. Huang, H. Zhang, Y. J. Gong and F. F. Li, J. Chem. Phys. **124**, 094302 (2006).
- [22] Y. Z. Lan, W. D. Cheng, D. S. Wu, X. D. Li, H. Zhang and Y. J. Gong, Chem. Phys. Lett. **372**, 645 (2003).
- [23] P. P. Korambath and S. P. Karna, J. Phys. Chem. A **104**, 4801 (2000).
- [24] B. Champagne, M. Guillaume, D. Bégué, and C. Pouchan, J. Comp. Meth. Sci. Eng. **7**, 297 (2007).
- [25] A. Sieck, D. Porezag, Th. Frauenheim, M. R. Pederson and K. Jackson, Phys. Rev. A **56**, 4890 (1997).
- [26] P. Karamanis and J. Leszczynski, J. Chem. Phys. **128**, 154323 (2008).
- [27] P. Karamanis, D. Xenides, and J. Leszczynski, J. Chem. Phys. **129**, 094708 (2008).
- [28] P. Karamanis, D. Xenides, and J. Leszczynski, Chem. Phys. Lett. **457**, 137 (2008).
- [29] A. Krishtal, P. Senet, and C. V. Alsenoy, J. Chem. Phys. **133**, 154310 (2010).
- [30] P. Karamanis, P. Carbonnière, and C. Pouchan, Phys. Rev. A **80**, 053201 (2009).
- [31] P. Karamanis, D. Bégué, and C. Pouchan, J. Chem. Phys. **127**, 094706 (2007).
- [32] P. Karamanis, C. Pouchan, C. A. Weatherford, and G. L. Gutsev, J. Phys. Chem. C **115**, 97 (2011).
- [33] J. L. Brédas, C. Adant, P. Tackx, A. Persoons, and B. M. Pierce, Chem. Rev. **94**, 243 (1994).
- [34] J. Wang, L. Zhu, X. Zhang, and M. Yang, J. Phys. Chem. A **112**, 8226 (2008).
- [35] H. Xu, Z. Li, F. Wang, D. W. K. Harigaya, and F. Gu, Chem. Phys. Lett. **454**, 323 (2008).
- [36] G. U. Gamboa, P. Calaminici, G. Geudtner, and A. M. Köster, J. Phys. Chem. A **112**, 11969 (2008).
- [37] P. Pradhan and A. K. Ray, J. Mol. Struct.(THEOCHEM) **716**, 109 (2005).
- [38] J. L. Deng, K. H. Su, X. Wang, Q. F. Zeng, L. F. Cheng, Y. D. Xu, and L. T. Zhang, Eur. Phys. J. D **49**, 21 (2008).
- [39] X. F. Duan and J. Wei and L. Burggraf and D. Weeks, Comp. Mater. Sci., **47**, 630 (2010).
- [40] G. Froudakis and A. Zdetsis and M. Mühlhäuser and B. Engels and S. D. Peyerimhoff, J. Chem. Phys. **101**, 6790 (1994).
- [41] I. L. Alberts, R. S. Grev, and H. F. Schaefer III, J. Chem. Phys. **93**, 5046 (1990)
- [42] M. C. McCarthy, A. J. Apponi, and P. Thaddeus, J. Chem. Phys. **110**, 10645 (1999)
- [43] M. C. McCarthy, A. J. Apponi, and P. Thaddeus, J. Chem. Phys. **111**, 7175 (1999)
- [44] J. M. Rintelman and M. S. Gordon, J. Chem. Phys. **115**, 1795 (2001)
- [45] K. W. Sattelmeyer and H. F. Schaefer III, J. Chem. Phys. **116**, 9151 (2002)
- [46] J. O. Hirschfelder and C. F. Curtis and R. B. Bird, Molecular Theory of Gases and Liquids, Wiley, New York, 1954, p950.
- [47] G. Maroulis, J. Phys. Chem. **100**, 13466 (1996).
- [48] M. A. Castro and S. Canuto, Phys. Rev. A **48**, 826 (1993).
- [49] M. J. Frisch, G. W. Trucks, H. B. Schlegel *et al.*, Gaussian 03, Revision D.01, Gaussian, Inc., Wallingford, CT, **2004**.
- [50] P. Fuentealba, Phys. Rev. A, **58**, 4232 (1998)
- [51] J. L. Wang, M. L. Yang, G. H. Wang, and J. J. Zhao, Chem. Phys. Lett. **367**, 448 (2003).
- [52] F. D. Proft, N. Sablon, D. J. Tozer, and P. Geerlings, Faraday Discuss. **135**, 151 (2007).

- [53] P. K. Chattaraj and S. Sengupta, J. Phys. Chem. **100**, 16126 (1996).
- [54] U. Hohm, J. Phys. Chem. A **104**, 8418 (2000).
- [55] R. G. Parr and P. K. Chattaraj, J. Am. Chem. Soc. **113**, 1854 (1991).
- [56] D. R. Kanis, M. A. Ratner, and T. J. Marks, Chem. Rev. **94**, 195 (1994).
- [57] J. L. Brédas, Science **263**, 487 (1994).
- [58] S. Hunsicker and R. O. Jones, J. Chem. Phys. **105**, 5048 (1996).
- [59] M. Gomei, R. Kishi, A. Nakajima, S. Iwata, and K. Kaya, J. Chem. Phys. **107**, 10051 (1997).
- [60] Z. Y. Jiang, X. H. Xu, H. S. Wu, and Z. H. Jin, J. Phys. Chem. A **107**, 10126 (2003).
- [61] M. N. Huda and A. K. Ray, Phys. Rev. A **69**, 011201 (2004).
- [62] J. Y. Hou and B. Song, J. Chem. Phys. **128**, 154304 (2008).